

## Temperature and magnetic field dependence of the electronic and lattice conductivities of tin from 1.3 to 6°K†

J. R. Pernicone and P. A. Schroeder

Department of Physics, Michigan State University, East Lansing, Michigan 48824

(Received 19 August 1974)

Extensive results are presented for the measurement of the components of the electrical- and thermal-resistivity tensors of pure tin in transverse magnetic fields up to 100 kG. The temperature dependence was studied between 1.5 and 6 K. From the thermal-resistivity measurements, the lattice conductivity of tin has been extracted. The results indicate that the lattice conductivity in the basal plane is significantly different from that obtained from dilute alloys. To study the temperature dependence of the electronic, electrical, and thermal conductivities it is necessary to neglect certain terms which arise in the inversion of the resistivity tensors. Within this approximation the temperature dependences are in agreement with Wagner's suggestion that the conductivities in the magnetic field should be simply related to the resistivities in zero field. The Lorenz number in a magnetic field is found to be field independent at high fields, and an increasing function of temperature.

### I. INTRODUCTION

In zero magnetic field the electron thermal conductivity of a pure metal is  $\sim 10\,000$  times the lattice conductivity. To measure the lattice conductivity the electronic component must somehow be reduced to the same order of magnitude as the lattice component, without at the same time affecting the latter. This has been done in the past by alloying<sup>1-4</sup> or by measuring the conductivity in the superconducting state.<sup>5,6</sup> However, it is also well known<sup>7,8</sup> that the electronic thermal conductivity can be very substantially reduced by the application of strong magnetic fields to a compensated metal (provided the angle between the current and the direction in  $k$  space of any open orbits excited does not approach  $90^\circ$ ), or to an uncompensated metal in a direction in which open orbits are excited. The lattice conductivity can then be extracted. This method has been used recently by Gorter and Noor-dermeer<sup>5</sup> on Ga, Long<sup>9</sup> and Wagner<sup>10</sup> independently on W, and Natarajan and Chari<sup>11</sup> on Rh. In the present work we apply the method to the measurement of the lattice thermal conductivity of tin—one of the few compensated simple polyvalent metals. Previous work on the lattice thermal conductivity of Sn includes that of Gueths *et al.*<sup>6</sup> and of Karamargin *et al.*<sup>12</sup> The former employed the superconducting thermal conductivity in a "universal-curve" type of analysis to deduce that the lattice conductivity in the normal state  $\kappa_g$  is proportional to  $T^{2.21 \pm 0.04}$  and to  $\rho_0^{-(0.21 \pm 0.04)}$ , where  $\rho_0$  is the residual resistivity. On the other hand, Karamargin *et al.* reduce the electronic thermal conductivity of tin by alloying with cadmium, and from their measurements obtain the lattice conductivity of the alloys. Then, assuming that between 4.5 and 12°K the phonon-electron scattering is the dominant scattering mechanism, they obtain the relation

$$\kappa_g = 1.5 \times 10^{-4} T^2 \text{ W cm}^{-1} \text{ K}^{-1}$$

for orientations close (within  $13^\circ$ ) to the basal plane.

In the course of our measurements of the lattice conductivity, the total thermal conductivity of tin has been measured over a range of temperatures and magnetic fields. It is of interest to see if the electronic-thermal-conductivity part of these data fits present theory of the temperature and field dependence. We will see in the theoretical section II, that tin is not the best material for this purpose, because its tetragonal structure precludes certain simplifications of the thermal-resistivity tensor. However, the analysis of our data in Secs. VA and VB appear to justify the neglect of certain terms in the tensor.

### II. THEORY

#### A. Lattice conductivity

Assume measurements are performed on a long thin crystal whose geometrical axis lies along the  $X$  axis. The transverse magnetic field is in the direction of the  $Z$  axis. The quantities measured are  $P_x$  the rate of flow of heat energy along the  $X$  axis and  $(\nabla T)_x$ , the  $X$  component of the temperature gradient. Since

$$\nabla T = A \overleftrightarrow{W} \cdot \vec{P}, \quad (1)$$

where  $\overleftrightarrow{W}$  is the thermal-resistivity tensor, and  $A$  is the cross-sectional area of the sample, it follows that essentially we determine  $W_{xx}$ . The total  $\vec{P}_T$  is just the sum of the powers conveyed by the electrons ( $\vec{P}_e$ ) and these conveyed by the lattice ( $\vec{P}_L$ ). For the present geometry it follows from Eq. (1) that

$$\frac{1}{W_{Txx}} = \frac{1}{W_{e_{xx}}} + \frac{1}{W_{L_{xx}}}, \quad (2)$$

where  $\vec{W}_T$ ,  $\vec{W}_e$ , and  $\vec{W}_L$  are the total, electronic, and lattice thermal-resistivity tensors, respectively.

At zero field, for a pure metal,

$$W_{T_{xx}} \sim W_{e_{xx}},$$

and information on the lattice conductivity cannot be obtained. To see what happens in the high-field region we must consider further the various transport-property tensors. First the electrical-conductivity and resistivity tensors for a compensated metal without open orbits are, respectively,

$$\vec{\sigma} = \begin{pmatrix} a_{xx}B^{-2} & a_{xy}B^{-1} & a_{xz}B^{-1} \\ -a_{xy}B^{-1} & a_{yy}B^{-2} & a_{yz}B^{-1} \\ -a_{xz}B^{-1} & -a_{yz}B^{-1} & a_{zz} \end{pmatrix}, \quad (3)$$

$$\vec{\rho} = \begin{pmatrix} b_{xx}B^2 & b_{xy}B^2 & b_{xz}B \\ -b_{xy}B^2 & b_{yy}B^2 & b_{yz}B \\ -b_{xz}B & -b_{yz}B & b_{zz} \end{pmatrix}, \quad (4)$$

where  $a_{ij}$  and  $b_{ij}$  are independent of the magnetic field  $B$ . For elastic scattering only, the Wiedemann-Franz law is expected to hold, and

$$\kappa_{xx}/\sigma_{xx}T = L_0, \quad (5)$$

where the Lorenz number  $L_0$  is independent of field and temperature.<sup>13</sup> If

$$\kappa_{ij} = 1/W_{ij}, \quad \sigma_{ij} = 1/\rho_{ij} \quad (6)$$

(which is generally not the case), then for elastic scattering

$$\rho_{xx}/W_{e_{xx}}T = L_0,$$

and we deduce from Eqs. (4) and (5) that

$$W_{e_{xx}} \propto B^2. \quad (7)$$

In actual practice the scattering will not be all elastic in the region in which we perform measurements, nor will Eq. (6) be strictly true. Despite this we expect (7) to be essentially correct in that  $W_{e_{xx}}$  should increase rapidly with  $B$ . Under these circumstances, as  $B \rightarrow \infty$ , we expect from Eq. (2) that

$$1/W_{T_{xx}} \rightarrow 1/W_{L_{xx}},$$

or, in words, at a sufficiently high magnetic field the measured thermal resistance is the lattice thermal resistance. This, of course, assumes that  $W_{L_{xx}}$  does not itself appreciably vary with  $B$ . We will initially assume that  $W_{L_{xx}}$  is independent of  $B$ . Then

$$\vec{W}_L = \begin{pmatrix} W_{L_{xx}} & 0 & 0 \\ 0 & W_{L_{yy}} & 0 \\ 0 & 0 & W_{L_{yy}} \end{pmatrix}$$

for the  $X$  axis along the fourfold  $\langle 001 \rangle$  principal axis. It follows that

$$\kappa_{L_{xx}} = 1/W_{L_{xx}}, \quad (8)$$

and  $\kappa_{L_{xx}}$  can therefore be determined from the thermal resistivity. Equations (2), (7), and (8) together give

$$1/W_{T_{xx}} = E/B^2 + \kappa_{L_{xx}}, \quad (9)$$

where  $E$  is a constant.

Similarly, if the  $X$  direction is in the basal plane, and if the direction of the field is chosen so that

$$\rho_{xx} \sim W_{e_{xx}} \sim B^2,$$

then we measure the second component of the lattice thermal conductivity tensor, again because  $W_{L_{ij}} = 1/\kappa_{L_{ij}}$  if the tensor is referred to its principle axes. We shall make use of Eq. (9) in the analysis of our results. However, we shall see that in practice the exponent of  $B$  may vary from 2.

Note that if  $\vec{\kappa}_L$  is indeed independent of magnetic field the same value of  $\kappa_L$  measured in the  $\langle 001 \rangle$  direction should be obtained for all transverse directions of the magnetic field. The same applies to  $\kappa_L$  measured in the basal plane.

#### B. Temperature dependence of the lattice conductivity

The lattice thermal conductivity for a metal in zero magnetic field and limited by phonon-electron interactions has been calculated by Klemens<sup>14,15</sup> for  $T \ll \Theta$ ,

$$\kappa_L = 313\kappa_i(T)(T/\Theta)^4 N_a^{-4/3}, \quad (10)$$

where  $\Theta$  is the Debye temperature,  $N_a$  is the number of electrons per atom, and  $\kappa_i$  is the ideal electronic thermal conductivity in zero field. Klemens assumes a spherical energy surface, a Debye model, that all the lattice modes—transverse as well as longitudinal—interact equally strongly with the conduction electrons, and that  $U$  processes in the phonon-electron interaction can be ignored. The expression is generally verified by experiments on alloys of copper, silver, and gold, where it is possible to separate the electron and lattice thermal conductivities.<sup>16</sup> For sufficiently low temperatures<sup>15</sup>

$$\kappa_i(T) \propto (\Theta/T)^2,$$

and therefore

$$\kappa_L \propto T^2/\Theta^2. \quad (11)$$

#### C. Temperature variation of $\kappa_{e_{xx}}$ and $\sigma_{xx}$ in a magnetic field

By comparison of expressions for  $\rho_{xx}$  and  $W_{xx}$  obtained from the Kohler Variational principle with expressions for  $\sigma_{xx}(B)$  and  $\kappa_{e_{xx}}(B)$  derived from semiclassical magnetoconductivity theory, Wagner<sup>17</sup>

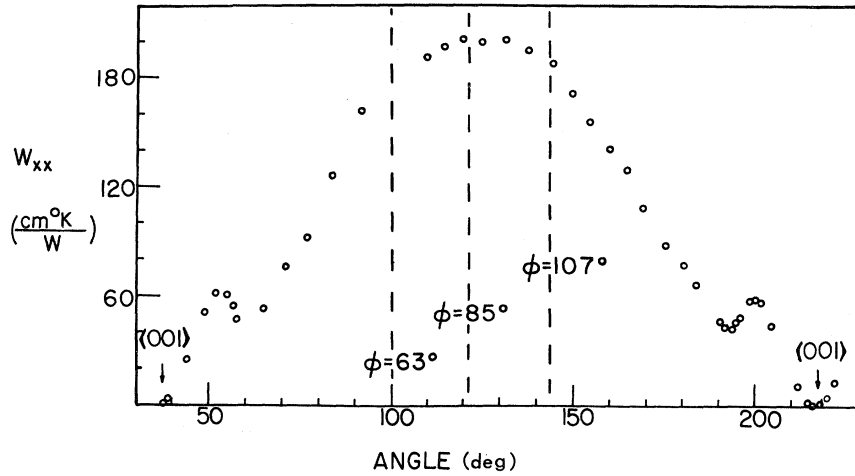


Fig. 1. Transverse thermal magnetoresistance for Sn crystal oriented in the basal plane plotted vs the angle of the magnetic field in a plane perpendicular to the basal plane.  $\phi$  is the angle measured from the  $\langle 001 \rangle$  direction.

concludes that it "may be reasonable to expect" that in the high-field limit, and for compensated metals,

$$\sigma_{xx}(B) \sim \rho_{xx}(0)$$

and

$$\kappa_{e_{xx}}(B) \sim T^2 W_{xx}(0),$$

where  $\rho_{xx}(0)$  is the zero-field electrical resistivity and  $W_{xx}(0)$  is the zero-field thermal resistivity. If we assume further that where  $c_1, c_2$  are constants and the first and second terms on the right-hand side correspond with impurity and phonon scattering, respectively, then it follows that

$$\sigma_{xx}(B) \sim a_1 + a_2 T^5,$$

where  $a_1$  and  $a_2$  are constants. If

$$\rho_{xx} \gg \frac{\rho_{xy}^2 \rho_{zz} + \rho_{xz}^2 \rho_{yy}}{\rho_{yy} \rho_{zz} + \rho_{zy}^2}, \quad (12)$$

then

$$1/\rho_{xx} - \sigma_{xx}(B) \sim a_1 + a_2 T^5. \quad (13)$$

Similarly, if we assume  $W_{xx}(0) = c_3/T + c_4 T^2$ , where again  $c_3$  and  $c_4$  are constants and the  $c_3/T$  term arises from impurity scattering, and the  $c_4 T^2$  term arises from phonon scattering, and if, furthermore, we make a similar assumption to Eq. (12), then

$$\kappa_{e_{xx}}(B) \sim a_3 T + a_4 T^4. \quad (14)$$

$a_1, a_2, a_3, a_4$  are constants in the above expressions.

In this work we attempt first to separate the lattice thermal conductivity by application of a high magnetic field, using Eq. (9). We also seek to verify the temperature dependences of  $\kappa_L, \rho_{xx}$ , and  $\kappa_{e_{xx}}$  given in Eqs. (11), (13), and (14), assuming that Eq. (12) holds.

### III. EXPERIMENTAL

The tin single crystals were grown by seeding in the desired orientation in a horizontal optically heated zone refiner. Thereafter they were cut to appropriate size. Samples for use in the electromagnet (up to 21 kG) were about 7 cm long and 3 mm<sup>2</sup> in cross section. Those for use in the superconducting solenoid were about 3 cm long. The residual-resistance ratio of all samples was at least 30 000. Samples were made with the length of the crystal within 3° of the  $\langle 001 \rangle$  direction, and of the basal plane. For the  $\langle 001 \rangle$  crystals the field was directed in the  $\langle 001 \rangle$  plane 30° from  $\langle 100 \rangle$ , where, according to Woollam<sup>18</sup> the magnetoresistance reaches a maximum. For the crystals oriented in the basal plane, the thermal magnetoresistance at a field of 20 kG was measured as a function of the angle  $\phi$ , the magnetic field made with the  $\langle 001 \rangle$  direction in a plane perpendicular to the basal plane. This is shown in Fig. 1. Measurements were performed at the positions indicated, where  $\phi = 63^\circ, 85^\circ, \text{ and } 107^\circ$ .

Resistivities were measured from 1.5 to 4.2°K in fields up to 21 kG (electromagnet) supplemented by some measurements at 4.2°K in the superconducting solenoid. A standard four-probe technique was used with the voltage probes soldered to the crystal, one third of the crystal length from each end. The thermal-resistivity measurements were performed by the conventional method of measuring the temperature difference produced across a long thin sample when a measured heating power was applied to a heater at one end of the crystal.

Carbon resistors were used as the thermometers. The method for correcting for their field dependence is outlined in Appendix A. By the application of the magnetic field we reduce the thermal conductivity by a factor  $\sim 5000$ . The experimental problems are not therefore those normally asso-

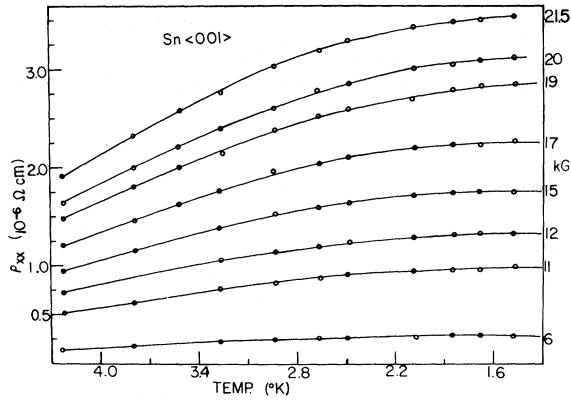


FIG. 2.  $\rho_{xx}$  plotted as a function of temperature for various magnetic fields. The  $\langle 001 \rangle$  axis of the crystal is in the direction of current flow. The direction of  $\vec{B}$  is  $30^\circ$  from  $\langle 100 \rangle$ .

ciated with a high-conductivity metal, but those associated with a good thermal insulator—namely, that there should be no parallel leakage paths for the heat to flow along. Precautions were therefore made to preclude the possibility that appreciable heat could be (a) radiated from the heater, (b) conducted by the remanent gas in the high-vacuum system, and (c) conducted from lead wires from heaters or thermometers. Also the thermometers were self-supporting—in the solenoid experiments the carbon resistors were placed in copper holders. Wrapped around and soldered to the thermometer holders with indium was a length of No. 30 Standard Wire Gauge copper wire. One end of this wire was then delicately soldered with indium to the crystal.

Manganin wires were used as current and voltage leads. In the electromagnet experiments the wire lead of the carbon resistor was directly soldered with Rose's alloy to the crystal. A check was made to see if there was an appreciable Righi-Leduc component in the measured temperature due to the thermometers not being accurately aligned by reversing the field and repeating the measurements. No appreciable difference was observed. Appreciable temperature differences were used, from 100 mK to  $1^\circ\text{K}$ , in both the solenoid and the electromagnet. The justification for this and the method used for finding the temperature corresponding to a given  $W_{xx}$  is outlined in Appendix B.

#### IV. RESULTS

In Fig. 2 we show the electrical magnetoresistance of the  $\langle 001 \rangle$ -orientation crystal as a function of temperature for various magnetic fields. Results for the crystal with the current in the basal plane are shown in Fig. 3 for  $\phi = 85^\circ$ . Note that for compensated metals in a magnetic field  $\rho_{xx}$  decreases with temperature in the high-field region, and tends to become constant at the lower temperatures.

In Fig. 4 we show some typical results of  $1/W_T$  versus temperature for the crystal oriented in  $\langle 001 \rangle$  obtained in the superconducting solenoid. Similar data for the basal plane ( $\phi = 85^\circ$ ) is shown in Fig. 5, using the electromagnet.

#### V. DATA ANALYSIS AND DISCUSSION

##### A. Electrical resistivity

From the data of Figs. 2 and 3,  $\rho_{xx}$  may be obtained as a function of field at specific tempera-

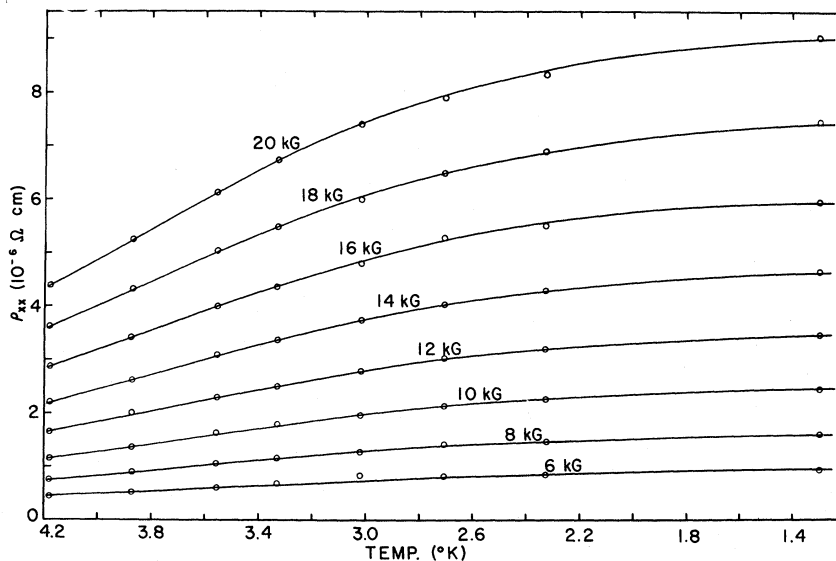


FIG. 3.  $\rho_{xx}$  plotted as a function of temperature for various magnetic fields. The current is in the basal plane.  $\phi = 85^\circ$ . (See Fig. 1).

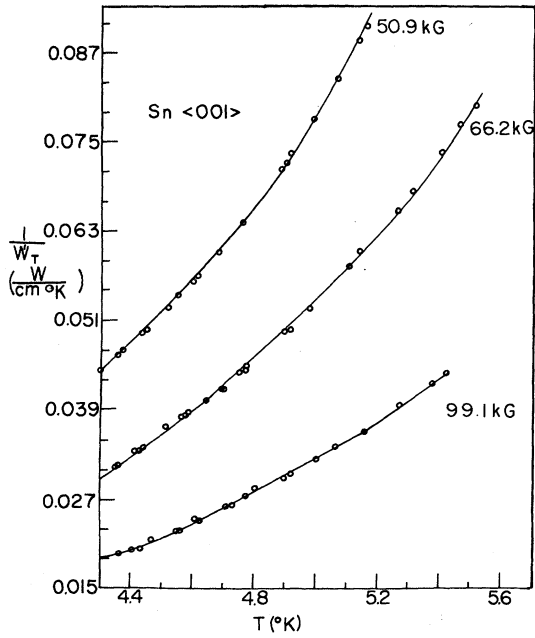


FIG. 4.  $1/W_T$  vs  $T$  for  $\langle 001 \rangle$ -oriented crystal.

tures. Plots of  $\rho_{xx}$  versus  $B^2$  are shown in Fig. 6 for  $\langle 001 \rangle$  crystal. As a more precise check on the power dependence of  $B$ ,  $\rho_{xx}$  was least-square fitted to the expression [see Eq. (4)]

$$\rho_{xx} = bB^p$$

for the data in Fig. 2 and for a sample measured in the superconducting solenoid for fields from 20 to 100 kG. The results of this analysis are given in Table I. Essentially,  $p$  is independent of temperature but has a mean value of 1.93, somewhat less than the theoretical value of 2.

In Fig. 7 we show a plot of  $1/\rho_{xx}$  vs  $T^5$  from 1.5 to 3.5 °K. The range is somewhat narrow but does indicate the approximate validity of Eq. (13). For a field of 21.5 kG, a least-squares fit to

$$1/\rho_{xx} = a_1 + a_2 T^q$$

gives a best value of  $q = 4.6$ . The fact that Eq. (13) is obeyed quite well suggests that Eq. (12) must also be approximately true. There is no *a priori* reason why Eq. (12) should be satisfied. All terms in this expression go as  $B^2$ , and there are no symmetry conditions which simplify it. As  $T \rightarrow 0$ ,  $1/\rho_{xx} \rightarrow a_1$ , the impurity scattering component which corresponds to the almost constant low temperature  $\rho_{xx}$  in Figs. 2 and 3. This tells us that below  $\sim 2.5$  °K impurity scattering predominates.

The analysis for the crystal oriented in the basal plane is similar. In Table II we show the coefficients in the least-squares fit of the data to  $\rho_{xx} = bB^p$  for  $\phi = 85^\circ$  and  $63^\circ$ . Further experiment indicates

$p$  is independent of field from 6 to 20 kG.  $p$  is clearly less than the theoretical value of 2, and, further, it changes with field direction. In Fig. 8 we show  $1/\rho_{xx}$  plotted as a function of  $T^{4.6}$ . Again

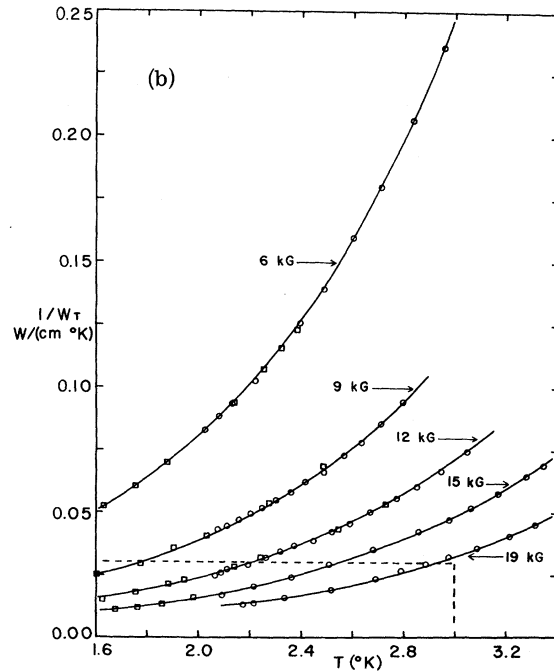
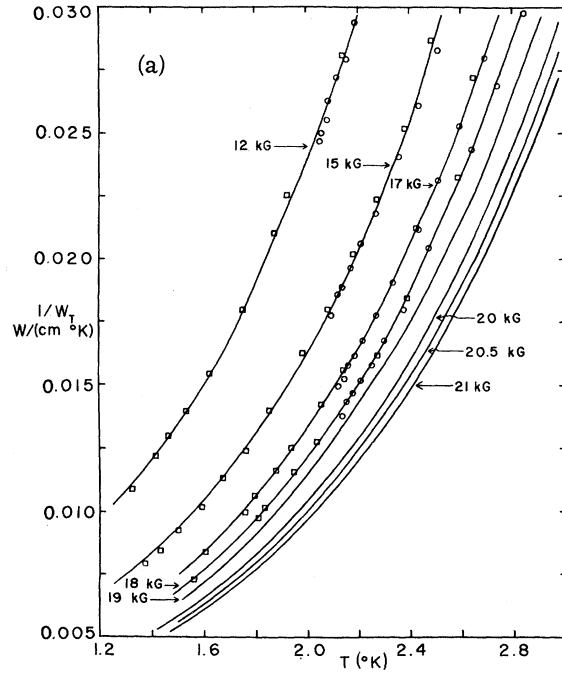
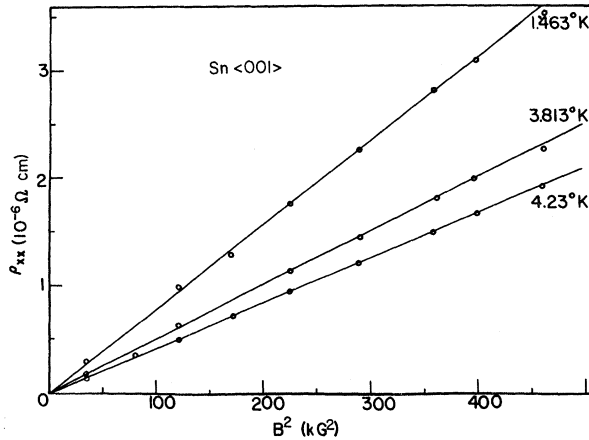


FIG. 5.  $1/W_T$  vs  $T$  for the geometrical crystal axis in the basal plane. The region covered by (a) is indicated by the dashed lines in (b).

FIG. 6.  $\rho_{xx}$  vs  $B^2$  for  $\langle 001 \rangle$ -oriented crystal.

the results indicated that Eqs. (12) and (13) are approximately true.

#### B. Thermal resistivity

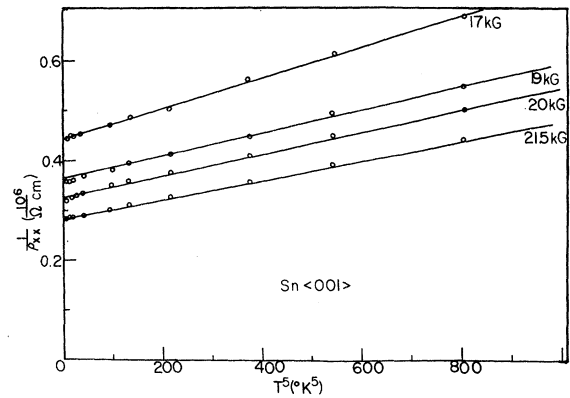
We test Eq. (9) by plotting  $1/W_{T_{xx}}$  vs  $B^{-2}$ . The results for the  $\langle 001 \rangle$  oriented crystal, using fields up to 100 kG in the superconducting solenoid, are shown in Fig. 9. The fit appears to be very good, and it would seem that all one has to do is pick the values of  $\kappa_L$  off the intercepts. Note, for future reference, that the extrapolation in this set of experiments involves a factor of between 2 and 3 between the last measured value of  $1/W_{T_{xx}}$  and the extrapolated  $\kappa_L$ . Unfortunately, this pleasant state of affairs vanishes when the data are least-square fitted to

$$1/W_{T_{xx}} = \kappa_L + EB^s. \quad (15)$$

Then it is discovered that the best value of  $s$  is not 2, and, furthermore, it varies with temperature,

TABLE I. Coefficients  $b$  and  $p$  in the least-squares fitting of the data for  $\rho_{xx}$  in the  $\langle 001 \rangle$  direction to  $\rho_{xx} = bB^p$ .

Temperature ( $^{\circ}$ K)	$b$ ( $10^{-11} \Omega \text{ cm}/(\text{kG})^p$ )	$p$
4.23	5.2	1.92
3.81	6.1	1.93
3.52	6.6	1.94
3.26	8.1	1.91
2.93	8.1	1.93
2.66	9.1	1.91
2.48	8.79	1.93
2.08	8.35	1.97
1.83	9.54	1.93
1.67	9.31	1.94
1.44	9.32	1.94
Solenoid		
4.20	0.052	1.93

FIG. 7.  $1/\rho_{xx}$  plotted as a function of  $T^5$  for  $\langle 001 \rangle$ -oriented crystal.

as indicated in Table III. In this table we include some values ( $T = 2.2$ – $2.5$   $^{\circ}$ K) taken using the electromagnet. We see that for these latter measurements  $s$  is close to the theoretical high-field value of 2. This then suggests that for the higher-temperature measurements we should permit  $s$  in Eq. (15) to vary with  $B$ .

This we have attempted to do, but now serious problems arise, in that we have no independent knowledge, experimental or theoretical, of how  $s$  should vary with  $B$ . We can fit the data to various modifications of Eq. (15) which allow for field variation of  $s$ , and obtain better fits than Eq. (15) with  $s$  constant, but the value of  $\kappa_L$  obtained depends very sensitively on the modified form of Eq. (15) that we use. This then introduces a certain arbitrariness in the values of  $\kappa_L$  which is difficult to assess. With

TABLE II. Coefficients  $b$  and  $p$  in the least-squares fitting of the data for  $\rho_{xx}$  in the basal plane to  $\rho_{xx} = bB^p$ .

Temperature ( $^{\circ}$ K)	$b$	$p$
$\phi = 85^{\circ}$		
4.18	0.63	1.92
3.87	0.74	1.92
3.56	0.85	1.93
3.33	0.96	1.92
3.02	1.08	1.91
2.71	1.19	1.91
1.30	1.44	1.89
$\phi = 63^{\circ}$ (Second direction)		
4.18	0.75	1.82
3.87	0.89	1.81
3.56	0.99	1.82
3.33	1.11	1.81
3.02	1.23	1.81
2.71	1.31	1.81
1.30	1.48	1.81

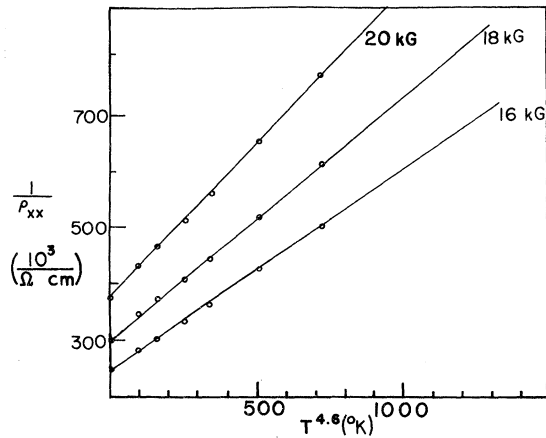


FIG. 8.  $1/\rho_{xx}$  as a function of  $T^{4.6}$  for a crystal oriented in the basal plane.

our present information we consider the analysis using Eq. (15) with  $s$  independent of  $B$  to be the most appropriate, but point out that considerable errors in the extrapolation process can arise. It is therefore very commendable that the extrapolation should be over as short a range as possible.

The electromagnet and solenoid data in Table III do not agree very well with each other. The difficulties arising from the variation of  $s$  with  $B$  are more pronounced in the solenoid data. On the other hand, the distance extrapolated is greater for the electromagnet data.  $\kappa_L$  (using Eq. (15) for extrapolation) is  $\approx \frac{1}{4}$  the lowest measured value of  $1/W_T$  for the solenoid, but is  $\approx \frac{1}{10}$  the lowest measured value of  $1/W_T$  for the electromagnet. For this reason we believe the solenoid results to be the more

TABLE III. Coefficients of  $E$  and  $s$  in the least-squares fitting of the data for  $1/W_{T_{xx}}$  in the  $\langle 001 \rangle$  direction to  $1/W_{T_{xx}} = \kappa_L + E B^2$ .

Temperature ( $^{\circ}$ K)	$s$	$E$	$\kappa_L$
6.00	-1.69	117.3	0.0162
5.70	-1.70	96.5	0.0145
5.40	-1.71	78.7	0.0128
5.10	-1.72	64.0	0.0113
4.80	-1.72	50.1	0.0095
4.50	-1.73	40.0	0.0081
4.20	-1.75	31.8	0.0068
2.50	-1.96	14.0	0.0041
2.40	-1.96	12.6	0.0036
2.30	-1.95	11.2	0.0030
2.20	-1.93	9.9	0.0022

reliable. Values for  $T > 2.5$   $^{\circ}$ K for the electromagnet results are not included in Table III because the uncertainty in the extrapolation procedure made values of  $\kappa_L$  from the measurements of little significance. A least-squares fit of the  $\kappa_L$  values of Table III to  $\kappa_L = dT^r$  for the solenoid data yields

$$\kappa_L = (2.03 \times 10^{-4}) T^{2.45}. \quad (16)$$

This is to be compared with the  $T^{2.21}$  dependence of Gueths *et al.* This relation, along with the experimental points in Table III, is shown in Fig. 10. A second graph showing the theoretical  $T^2$  normalized at the 5.1  $^{\circ}$ K point is also given. The departure of the low-temperature points from either of these curves we ascribe to the greater uncertainty in the extrapolation procedures for these points. We will come back to a discussion of the  $T^{2.45}$  dependence for  $\kappa_L$  after we have considered the results for the basal plane.

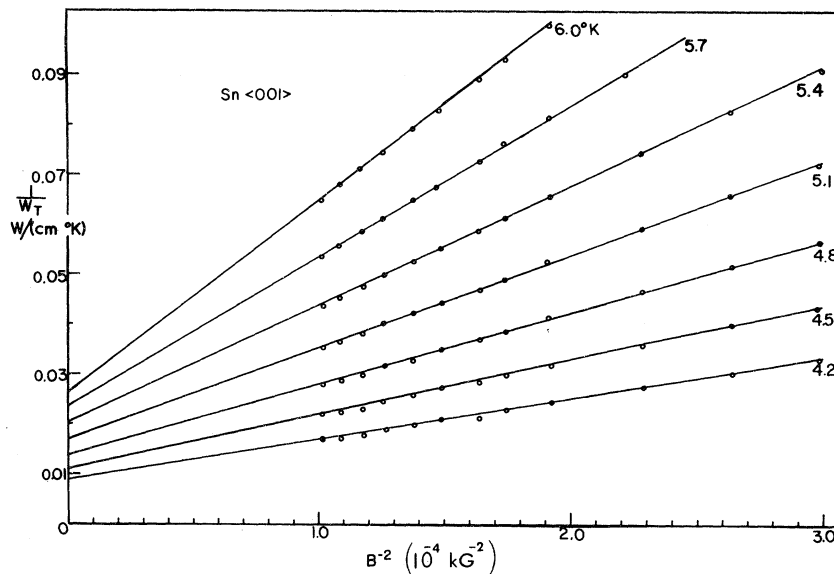


FIG. 9.  $1/W_T$  vs  $B^2$  for the  $\langle 001 \rangle$ -oriented crystal.

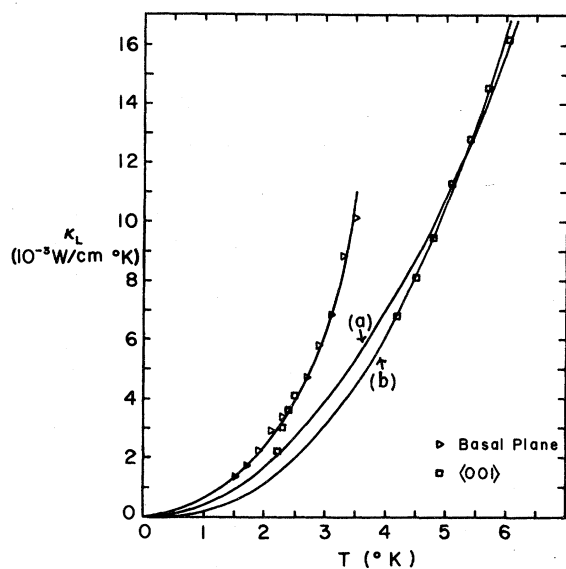


FIG. 10.  $\kappa_L$  as a function of  $T$ . Curve (a) is a  $T^2$  dependence normalized at the 5.1°K point. Curve (b) is Eq. (16).

The data for the variation of  $1/W_T$  with  $B^{-2}$  for the basal plane are shown in Fig. 11. There is a certain amount of nonlinearity for  $B < 10$  kG. The data were therefore fitted to Eq. (15), using  $B > 15$

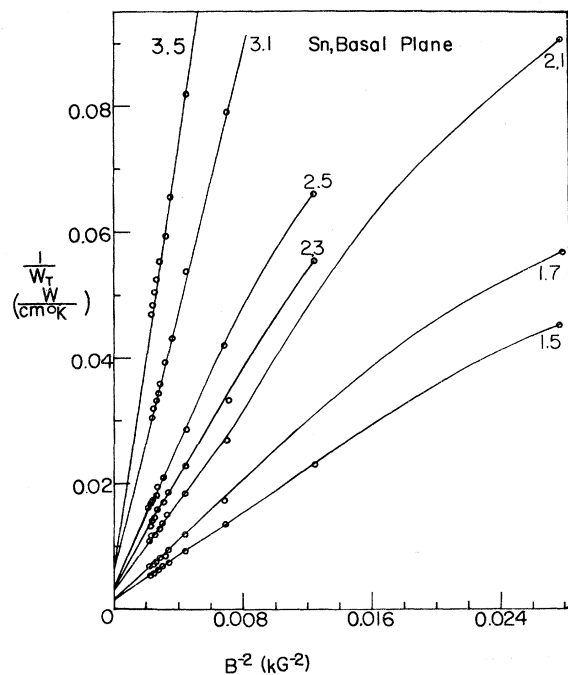


FIG. 11.  $1/W_T$  as a function of  $B^{-2}$  for the crystal oriented in the basal plane.  $\phi = 85^\circ$ .

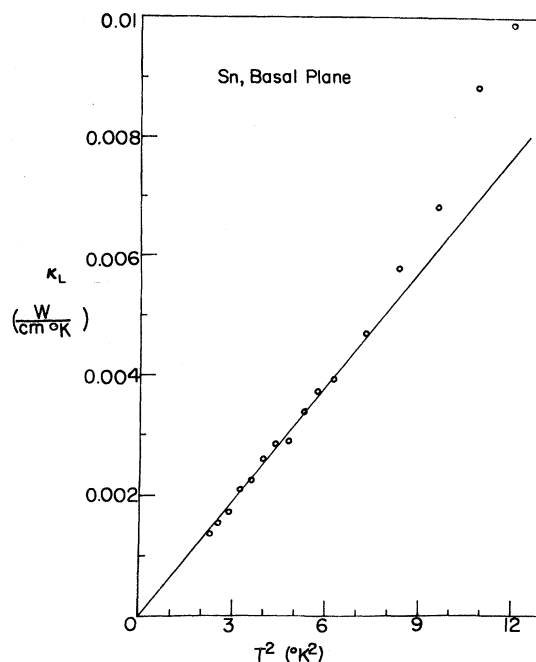


FIG. 12.  $\kappa_L$  vs  $T^2$  for the crystal oriented in the basal plane.  $\phi = 85^\circ$ .

kG, and  $\alpha = 2$ . Results for  $\kappa_L$  are shown in Fig. 12, plotted as a function of  $T^2$ . The data for  $\kappa_L$  are given in Table IV. The exponent for the lower portion of the graph is more correctly 2.1, but the main point at the moment is the departure of  $\kappa_L$  from a  $T^2$  dependence at  $T \sim 2.7^\circ\text{K}$ . We propose that this gross departure from a  $T^2$  law is associated with the sudden plunge in the Debye temperature for tin illustrated in Fig. 13.<sup>19</sup> Over a range of  $\sim 7^\circ\text{K}$ ,  $\Theta$  decreases by  $\sim 40\%$ . Equation (11) indicates that one might therefore expect a considerable increase of  $\kappa_L$  in this region. We propose that the rather high exponent of  $T$  in Eq. (16), which essentially comes from results in the 4–6°K region, may be associated with the same rapid variation of  $\Theta$ .

Our results for the basal plane are consistently about 4 times greater than those of Karamargin *et al.*<sup>12</sup> This discrepancy is well outside the range of experimental or extrapolation errors. There are two possibilities. Either the magnetic field does affect the lattice conductivity or else the true lattice thermal conductivity of the pure metal is not obtained from the  $T^2$  region of the alloy thermal conductivity. Regarding the former possibility, if  $\kappa_L$  depends on the magnetic field, we might expect it to vary with the direction of the field. With this in mind, measurements of the thermal conductivity were also made for  $\phi = 63^\circ$  and  $107^\circ$ . We show some of the data for the three angles in Fig. 14.



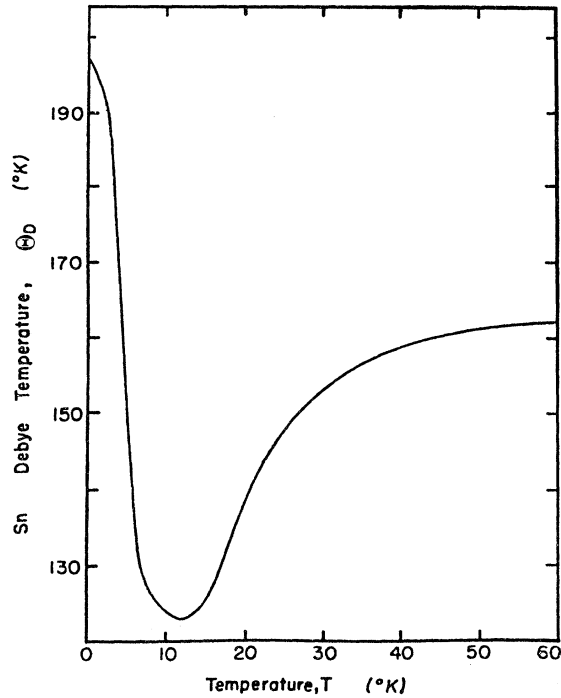


FIG. 13. Debye Temperature for tin as a function of temperature.

In this figure, lines have been drawn through the  $\kappa_L$  values derived for the  $\phi = 85^\circ$  measurements on the ordinate. In each case the line drawn is a reasonable one, but not necessarily the best fit. What this figure says is that within the experimental error we cannot detect a change of  $\kappa_L$  with field direction. This in turn is some evidence that  $\vec{\kappa}_L(B)$  is a two-component tensor typical of a tetragonal system. Regarding the second possibility, we note that the thermal resistance due to dislocations has the same  $T^2$  dependence as that produced by phonon-electron scattering.<sup>7,8,20</sup> Neither our method nor the alloying method will distinguish the component

TABLE IV. Lattice conductivity in the basal plane.

Temperature ( $^\circ\text{K}$ )	$\kappa_L$ ( $\phi = 85^\circ$ ) ( $\text{W}/\text{cm K}$ )
1.50	0.0014
1.70	0.0017
1.90	0.0023
2.10	0.0029
2.30	0.0034
2.50	0.0039
2.70	0.0047
2.90	0.0058
3.10	0.0068
3.30	0.0088
3.50	0.0101

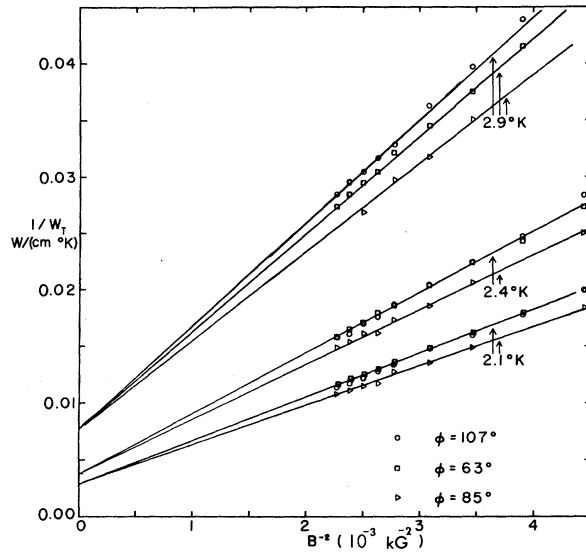


FIG. 14.  $1/W_T$  plotted as a function of  $B^2$  for a crystal in the basal plane.  $\phi = 63^\circ, 85^\circ, 107^\circ$ .

of the lattice thermal resistance arising from electron and dislocation scattering. It is conceivable that Karamargin's alloys, which were annealed for 350 h at  $170^\circ\text{C}$ , do retain a substantial concentration of dislocations, but this needs considerably more experimental work to verify.

We note from Eq. (10) that

$$\kappa_L \propto \kappa_i.$$

and we therefore might expect the anisotropies of  $\kappa_L$  and  $\kappa_i$  to be similar. From Fig. 10 we observe that

$$\kappa_{L_{\parallel}} \sim 1.9 \kappa_{L_{\perp}},$$

where the  $\perp$  and  $\parallel$  subscripts correspond to perpendicular and parallel to the  $\langle 001 \rangle$  direction. Karamargin's<sup>19</sup> measurements on  $\kappa_i$  for tin fairly close to the above directions ( $6^\circ$  and  $78^\circ$  from  $\langle 001 \rangle$ ) yield

$$\kappa_{i_{\parallel}} \sim 1.45 \kappa_{i_{\perp}}.$$

The correspondence is satisfactory considering that the crystal orientations are not identical and the difficulties in extrapolation to obtain  $\kappa_L$ .

#### C. Temperature dependence of the electronic thermal conductivity

We consider the temperature dependence of the electronic thermal conductivity by testing Eq. (14). To do so we have to assume  $\kappa_e(B) = 1/W_e(B)$ . Again we know of no simple justification for this. However in Figs. 15 and 16 we plot  $1/W_e(B)T$  as a function of  $T^3$  and find that for the  $\langle 001 \rangle$  the  $T^3$  dependence holds very well ( $T^{3.14}$  by least-squares fit). For

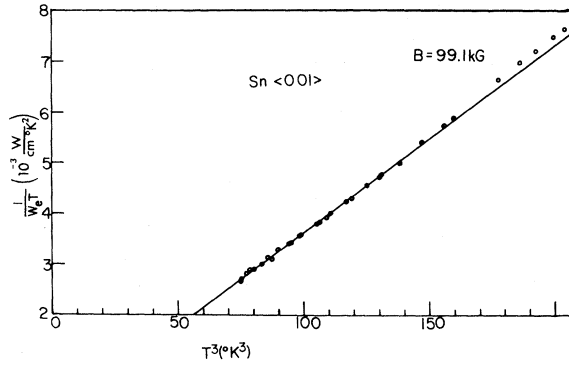


FIG. 15.  $1/W_e T$  plotted as a function of  $T^3$  for crystal oriented in  $\langle 001 \rangle$  direction.

the basal plane the  $T^3$  dependence is initially good at low temperatures, but at  $T \sim 2.7^\circ \text{K}$  there are significant departures which may also be associated with the rapid decrease in  $\Theta$  at this approximate temperature.

Finally, we consider what happens to our bogus Lorenz number

$$L(B) = \rho_{e_{xx}} / W_{e_{xx}} T$$

in a magnetic field. Again, this is only an approximation to the real Lorenz number

$$L = \sigma_{xx} / \kappa_{xx} T.$$

Our results indicate that  $L(B)$  is independent of  $B$  between 10 and 20 kG, within the experimental error for the basal plane. For the  $\langle 001 \rangle$  direction  $L(B)$  decreases  $\sim 10\%$  as  $B$  increases over the same range. In both cases the mean  $L(B)$  increases with temperature, as indicated in Fig. 17. The theory for the Lorenz number in a magnetic field is not well developed. However, for large values of  $B$  Sondheimer and Wilson<sup>21</sup> find that for a two-band model for a compensated metal

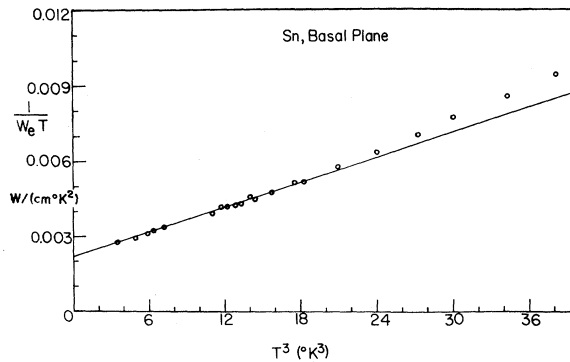


FIG. 16.  $1/W_e T$  plotted as a function of  $T^3$  for crystal oriented in the basal plane.

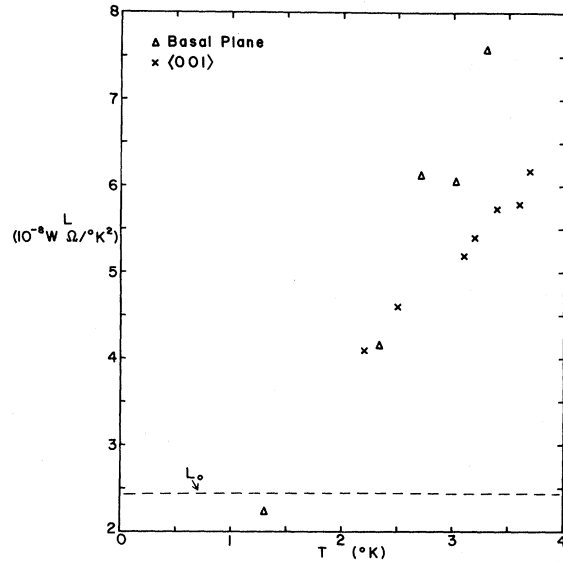


FIG. 17. Lorenz ratio in a magnetic field plotted as a function of temperature.  $L_0 = 2.445 \times 10^{-8} \text{ W Ohm / K}^2$  shown as dashed line.

$$L(B) = L_0^2 / L(0),$$

where  $L(0)$  is the Lorenz number in zero field. Generally, for a metal  $L(0)$  tends to  $L_0$  as  $T$  tends to  $0^\circ \text{K}$ , and decreases as  $T$  increases. On this basis we expect  $L(B) \rightarrow L_0$  as  $T \rightarrow 0^\circ \text{K}$  and  $L(B)$  to be an increasing function of  $T$ . The experimental results fit this observation in at least a qualitative sense.

## VI. CONCLUSIONS

(i) The lattice conductivity of tin has been measured by suppressing the electronic conductivity through the application of a high magnetic field. There are difficulties in the extrapolation procedure which probably limit the over-all accuracy in  $\kappa_L \sim \pm 10\%$ . It is important to decrease the range of the extrapolation as far as possible. This requires that  $\kappa_L / \kappa_E(B)$  should be maximized. From Eqs. (11) and (14) the condition for this is that

$$T^3 = a_3 / 2a_4,$$

where  $a_3$  and  $a_4$  have the same significance as in Eq. (14). For the sample in the basal plane at 20 kG, shown in Fig. 16, this yields  $T \sim 1.8^\circ \text{K}$ . This temperature is primarily determined by  $a_3$ , which appears in the term due to impurity scattering. The higher the impurity scattering, the higher the temperature at which the extrapolation conditions are best. In the extrapolation procedures, one must take into account the fact that the exponent of  $B$  in Eq. (9) may be different from 2.

(ii) Our values of  $\kappa_L$  in the basal plane are significantly different from those of Karamargin *et al.*,<sup>12</sup> obtained by alloying.

(iii) The temperature dependence of  $\kappa_L$  is close to the theoretical dependence. There is no conclusive evidence that  $\kappa_L$  depends on the direction of the magnetic field.

(iv) The temperature dependences of  $\rho_{xx}^{-1}$  and  $W_e^{-1}$  are close to the theoretical values. The implications are that Wagner's<sup>18</sup> supposition and Eq. (12) are essentially correct.

#### APPENDIX A

In this appendix we describe how the temperatures were measured in a magnetic field using carbon resistance thermometers. At zero field several calibration points were least-square fitted to the Clement-Quinnell<sup>22</sup> three-parameter equation

$$\ln R + A/\ln R = D + C/T.$$

The calibration points were obtained by measuring the vapor pressure of helium in the electromagnet experiments, and by using a calibrated germanium thermometer in the solenoid experiments.

At nonzero fields, in the electromagnet experiments, the constants in the Clement-Quinnell equation were reevaluated at each field at which thermal and electrical conductivity experiments were performed. This follows the suggestion of Neuringer and Shapira.<sup>23</sup> In the solenoid experiments which were performed above 4.2 °K, we could not use the vapor pressure of helium for temperature measurement in a magnetic field. Nor could we use germanium thermometers, which are well known to be strongly field dependent.

We define  $\Delta T$  as the error in measuring temperature in a magnetic field using the zero-field calibration. On studying the data of Neuringer and Shapira<sup>23</sup> we found (a) that  $\Delta T$  was approximately linearly dependent on  $T$  for  $T > 4.2$  °K and (b) that  $\Delta T$ , for several resistors of different values and for different fields, formed a family of nonintersecting curves. We measured  $\Delta T$  at 4.2 °K and used this family of curves to give us  $\Delta T$  at higher temperatures.

We believe that uncertainties in  $T_2 - T_1$ , taking into account errors in resistance measurement and errors caused by the lack of a precise resistance-temperature relation in a magnetic field, amounted to  $\pm 2$  mK at 4 K and  $\pm 10$  mK at 5.5 K in the solenoid experiments. For the electromagnet experiments it was  $\pm 3$  mK for all temperatures.

We should remark that there is a time drift with carbon resistors. Our standard practice was to leave the thermometers at 4.2 °K for 2 h before the calibration and measurements were commenced.

The most rapid part of the drift occurs within that time. Thereafter, errors from this cause become small compared with those mentioned above.

#### APPENDIX B

It is always difficult to make precise measurements of small differences in temperature—doubly so in a magnetic field. In this appendix we describe a method whereby this problem is avoided.

For heat transmission along the  $x$  axis only, Eq. (1) becomes

$$dT/W_{xx} = (dx/A)P_x,$$

where  $dT$  and  $dx$  are differentials. For finite  $T$  and  $x$ ,

$$\int_{T_1}^{T_2} \frac{dT}{W_{xx}} = P_x \int \frac{dx}{A} = P_x S, \quad (\text{B1})$$

where  $S$  is a geometrical factor (determined by comparison of the measured electrical resistance with the known electrical resistivity at room temperature).  $P_x S$  we regard as the quantity measured experimentally.

From the mean-value theorem there is a temperature  $T_E$  such that

$$\frac{1}{W_{xx}(T_E)}(T_2 - T_1) = \int_{T_1}^{T_2} \frac{dT}{W_{xx}} = P_x S. \quad (\text{B2})$$

If  $P_x S$  and  $T_2 - T_1$  are measured, we then get a value of  $W_{xx}(T_E)$ . It now remains to find  $T_E$ . We do this by an iterative procedure. First we assume  $T_E = \frac{1}{2}(T_1 + T_2) = T_A$ . We also need a mathematical expression relating  $1/W_{xx}$  to  $T$  over the small range considered. This relation need not have physical significance. The expression we use is

$$1/W_{xx} = aT^x, \quad (\text{B3})$$

where  $a$  and  $x$  are constants. We substitute the measured  $W_{xx}(T_E)$  for  $W_{xx}$  and  $T_A$  for  $T$  and perform a least-squares fit to obtain  $a$  and  $x$ . We now substitute (B3) into (B2) to obtain

$$\int_{T_1}^{T_2} \frac{dT}{W_{xx}} = a \int_{T_1}^{T_2} T^x dT = \frac{a}{x+1} (T_2^{x+1} - T_1^{x+1}) \quad (\text{B4})$$

and

$$\int_{T_1}^{T_2} \frac{dT}{W_{xx}} = (T_2 - T_1) A T_E^x. \quad (\text{B5})$$

From (B4) and (B5) we obtain a new value of  $T_E$ . The process can be repeated, but we have found that the convergence is very rapid and usually only one iteration is necessary.

†Supported by National Science Foundation.

- <sup>1</sup>W. R. G. Kemp, P. G. Klemens, R. J. Tainsh, and G. K. White, *Acta Metall.* 5, 303 (1957).
- <sup>2</sup>T. Olsen, *J. Phys. Chem. Solids* 12, 167 (1959).
- <sup>3</sup>R. Fletcher and D. Greig, *Philos. Mag.* 16, 303 (1967).
- <sup>4</sup>M. Garber, B. W. Scott, and F. J. Blatt, *Phys. Rev.* 130, 2188 (1963).
- <sup>5</sup>F. W. Gorter and L. J. Noordermeer, *Physica (Utr.)* 46, 507 (1970).
- <sup>6</sup>J. E. Gueths, P. L. Gabarino, M. A. Mitchell, P. G. Klemens, and C. A. Reynolds, *Phys. Rev.* 178, 1009 (1969).
- <sup>7</sup>J. M. Ziman, *Electrons and Phonons* (Oxford, London, 1960) p. 325.
- <sup>8</sup>P. G. Klemens, in *Handbuch der Physik*, edited by S. Flügge (Springer, Berlin, 1956), Vol. XIV, p. 261.
- <sup>9</sup>J. R. Long, *Phys. Rev. B* 3, 2476 (1971).
- <sup>10</sup>D. Wagner, *Phys. Rev. B* 5, 336 (1972).
- <sup>11</sup>N. S. Natarajan and M. S. R. Chari, *Indian J. Pure Appl. Phys.* 9, 439 (1971).
- <sup>12</sup>M. C. Karamargin, C. A. Reynolds, F. P. Eifschultz, and P. G. Klemens, *Phys. Rev. B* 6, 3624 (1972).
- <sup>13</sup>A. H. Wilson, *The Theory of Metals* (Cambridge U. P., Cambridge, England, 1954) p. 319.
- <sup>14</sup>P. G. Klemens, *Handbuch der Physik*, edited by F. Flügge (Springer, Berlin, 1956), Vol. XIV, p. 198.
- <sup>15</sup>P. G. Klemens *Thermal Conductivity*, edited by R. P. Tye (Academic, New York, 1969), Vol. 1, p. 34-36.
- <sup>16</sup>P. G. Klemens, in *Solid State Physics*, edited by F. Seitz and D. Turnbull (Academic, New York, 1958), Vol. 7, p. 1.
- <sup>17</sup>D. K. Wagner, thesis (Cornell University, 1971) (unpublished).
- <sup>18</sup>J. Woollam, *Phys. Rev.* 185, 995 (1969).
- <sup>19</sup>M. C. Karamargin, Ph.D. thesis (University of Connecticut, 1971) (unpublished).
- <sup>20</sup>M. A. Mitchell, P. G. Klemens, and C. A. Reynolds, *Phys. Rev. B* 3, 1119 (1971).
- <sup>21</sup>E. H. Sondheimer and A. H. Wilson, *Proc. Roy. Soc. A* 190, 435 (1947).
- <sup>22</sup>J. R. Clement and E. H. Quinnell, *Rev. Sci. Instrum.* 23, 213 (1952).
- <sup>23</sup>L. Neuringer and Y. Shapira, *Rev. Sci. Instrum.* 40, 1314 (1969).